Distribution of K X Rays as a Function of Mass and Atomic Number in the Spontaneous Fission of ^{252}Cf†

R. L. Watson
Department of Chemistry and Cyclotron Institute, Texas A & M University, College Station, Texas 77843 and Lawrence Radiation Laboratory, University of California, Berkeley, California 94720
and
R. C. Jared and S. G. Thompson
Lawrence Radiation Laboratory, University of California, Berkeley, California 94720
(Received 22 December 1969)

Measurements of the intensities of K x rays in coincidence with fission were carried out in an experiment in which the energies of complementary fission fragment pairs and K x rays were recorded event by event, using a multiparameter analyzer. Subsequent analysis of the data resulted in the determination of the x-ray intensities associated with intervals of fragment mass for each contributing element. Most probable charge and mass values for the emission of K x rays were determined, and it was found that these most probable masses could be used to adequately define the Z_p curve —without appreciable biasing due to details of nuclear structure. An examination of the effect of total kinetic energy on the x-ray distribution revealed a distinct enhancement of even-Z K x-ray contributions to the yields as the total kinetic energy increases. Apparent shifts in the values of most probable masses for the emission of K x rays were also observed as a function of total kinetic energy.

I. INTRODUCTION

Much interest has been directed, lately, toward the study of x rays emitted from primary fission fragments, mainly because of their usefulness in identifying fragment atomic numbers and because their intensities supply insight into level structure characteristics. Further impetus to studies of x-ray emission following fission is provided by the fact that in principle this process, even though it occurs long after fission, still contains valuable information relating back to the fission mechanism.

The application of x-ray measurements to the determination of the charge distribution in fission has been particularly intriguing. Several experiments have been reported in which the distribution of most probable nuclear charge has been studied by measuring K x-ray intensities along with the masses of the fragments from which they arise.[1,2] Unfortunately, such studies must rely upon the assumption that the K x-ray emission probability is either constant or no more than slowly varying as a function of fragment composition (i.e., Z and A). Subsequent experiments,[3] however, have shown that the K x-ray emission probability is not a slowly varying function of Z, especially for heavy fragments where a pronounced even-odd effect has been observed, and this effect has raised questions concerning the validity of the x-ray method for determining Z_p values.

Since these earlier studies of the intensity of x rays as a function of fragment mass, the resolution obtainable with Si(Li) x-ray spectrometers has improved to the point of making possible the determination of the individual intensities of K x rays associated with elements of each atomic number produced in fission. Along with this advance, comes the capability of investigating in more detail the intensities of x rays as a function of both fragment mass and atomic number in order to better interpret features relating to the determination of the charge distribution. One such study concerning K x rays emitted in the thermal-neutron-induced fission of ^{233}U, and ^{239}Pu has recently been reported by Glendenin *et al.*[4]

The data to be presented in this paper were obtained in a study of the low-energy transitions arising from the prompt deexcitation of fission fragments which is reported in the work of Watson *et al.*[5] Our purpose here is to further examine the applicability of high-resolution x-ray measurements as a means of defining features of the primary charge distribution and to investigate the effect of fragment total kinetic energy on the K x-ray spectra.

II. EXPERIMENTAL PROCEDURES

A schematic diagram of the experimental arrangement is shown in Fig. 1. A weightless amount of ^{252}Cf deposited onto a thin (~70 μg/cm^2) nickel foil and giving a fission rate of approximately 3.8×10^6 fissions per min was mounted coaxially between two phosphorus-diffused silicon fission fragment detectors. The fragment detectors were collimated to 15 mm in diam and operated at −50°C. One fission fragment detector (fragment 1

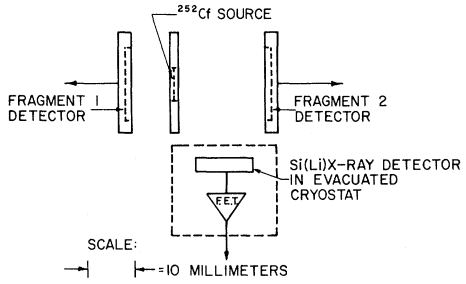

FIG. 1. Diagram of experimental configuration.

detector) was located 1.0 cm to the left of the fission source and the other (fragment 2 detector) was located 2.0 cm to the right of the fission source. Directly below and centered between the fission source and fragment 2 detector was located a lithium drifted silicon x-ray detector of dimensions 1 cm×1 cm×3 mm. This detector was mounted in a separate evacuated cryostat which was isolated from the main vacuum chamber by a 0.025-cm beryllium window and was located at a distance of 2.0 cm from the fission fragment detector-source axis. The x-ray detector and internally mounted field-effect transistor were operated at liquid-nitrogen temperature and gave an energy resolution of 0.75 keV full width at half maximum at 14 keV under the conditions of the experiment.

The three detector outputs were connected to low-noise preamplifiers and produced signals which were analyzed in a standard fast-slow coincidence system. In this system, it was required that an x ray be detected within a time interval of 100 nsec following fission and that two fission fragments be detected within the first 50 nsec of this time interval. Detector pulses which satisfied these requirements were routed to a multidimensional analyzer, digitized, and recorded onto magnetic tape event by event. (The electronic system is discussed in more detail in Ref. 5).

III. ANALYSIS AND RESULTS

The pulse heights which had been recorded on magnetic tape were subsequently processed on a CDC 6600 computer. In the computer processing, the fission-fragment pulse heights were transformed into fragment masses using a procedure described in Ref. 5, the x-ray pulse heights were sorted according to the mass of the fragment detected in fragment 2 detector and the total kinetic energy of the fission event into separate x-ray energy spectra for each 2-amu interval of mass and 15-MeV interval of total kinetic energy, and these "mass- and energy-sorted" x-ray spectra were plotted by a Cal Comp plotter.

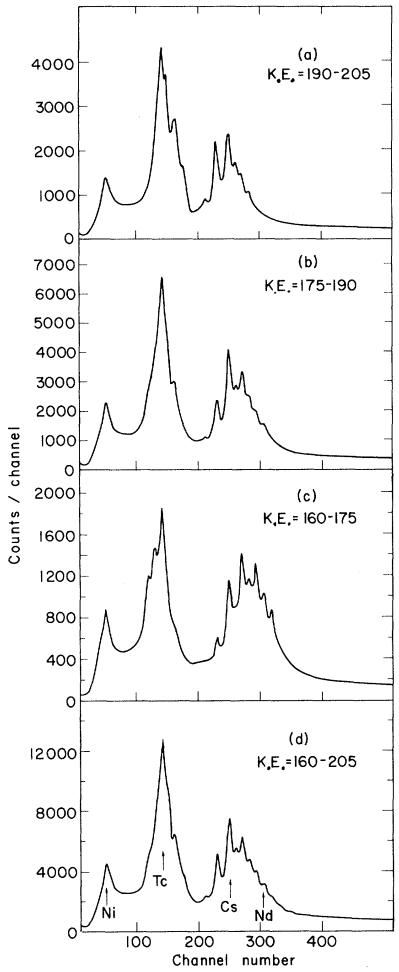

FIG. 2. K x-ray spectra (unsorted with respect to mass) for three intervals of total kinetic energy (a)–(c) and for the full range of total kinetic energy (d).

The spectra of K x rays summed over all mass intervals are shown in Fig. 2 for the three intervals of total kinetic energy (a) 190–205 MeV, (b) 175–190 MeV, (c) 160–175 MeV, and (d) 160–205 MeV – the K x-ray spectrum summed over all mass and total-kinetic-energy intervals. The marked changes of x-ray intensities exhibited by the spectra compared in Fig. 2 clearly illustrate the variation of fragment atomic number as a function of total kinetic energy. It can be seen that sorting the total x-ray spectrum (d) with respect to total kinetic energy, has the effect of accentuating the contributions to spectrum (a) of the light-fragment–high-Z, and heavy-fragment–low-Z elements, to spectrum (b) of the light- and heavy-fragment-intermediate-Z elements, and to spectrum (c) of the light-fragment–low-Z, and heavy-fragment–high-Z elements. This behavior is a reflection of the fact that the average

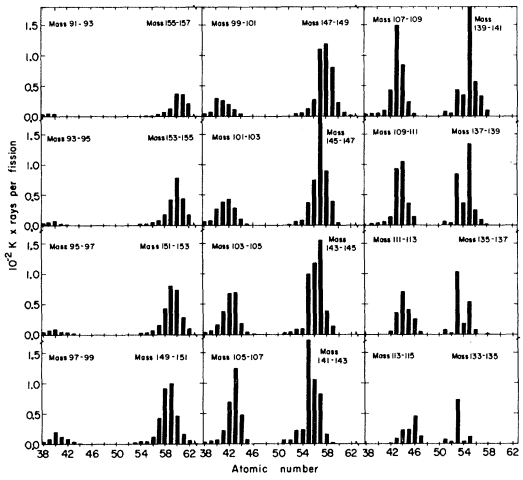

FIG. 3. The yields of K x rays for complementary intervals of fragment mass.

total kinetic energy increases as the atomic numbers of the light and heavy fragments approach $Z = 49$ and is in accord with the well-known variation of the average total kinetic energy with fragment mass.[6]

Each of the mass-sorted x-ray spectra was analyzed using a computerized least-squares peak fitting procedure (described in Ref. 3) to separate the individual x-ray distributions of each element from those of the other elements contributing to the same spectrum. In this way, the intensities of x rays associated with every mass and total-kinetic-energy interval were determined for each element. The x-ray intensities are shown in Fig. 3 as a function of atomic number for complementary heavy-fragment, light-fragment mass intervals, and are presented in a contour plot as a function of atomic number and neutron number in Fig. 4. In both Fig. 3 and Fig. 4, large variations are observed in x-ray intensities from one Z to the next. In Fig. 4, it is interesting to note the occurrence of the intense peaks centered at the odd-odd nuclei $^{108}_{43}Tc_{65}$, $^{136}_{53}I_{83}$, $^{140}_{55}Cs_{85}$, and $^{146}_{57}La_{89}$. In the work described in Ref. 5, it was found that these x-ray intensity peaks are accounted for by highly converted transitions occurring at 69, 59, 78, and 64 keV, respectively.

The absolute x-ray intensities summed over the whole range of total kinetic energy (160–205 MeV) are listed in Table I as a function of mass interval and atomic number. These absolute intensities are estimated to be accurate on the average to better than 20%, and the relative intensities to approximately 10%. The largest sources of error are associated with the varying detection geometry of x rays emitted at different points along the fragment flight path from source to detector and with the uncertainty arising from the peak fitting procedure. Measurements of average x-ray emission times in ^{252}Cf fission by Kapoor, Bowman, and Thompson[2] and by Dolce, Gibson, and Thomas,[7] however, have shown that most of the x rays are emitted between the times of 0.5 to 0.9 nsec after fission. Over this more restricted range of emission points, the *average* detection geometry varies by approximately 5.6%. The average detection geometry was determined by normalizing the total x-ray yields (summed over mass and kinetic energy) for Tc and Cs to those reported in Ref. 3. The average deviation of the other x-ray yields in the normalized distribution from the yields given in Ref. 3 was 10.2%.

Pursuing now the question of how best to relate

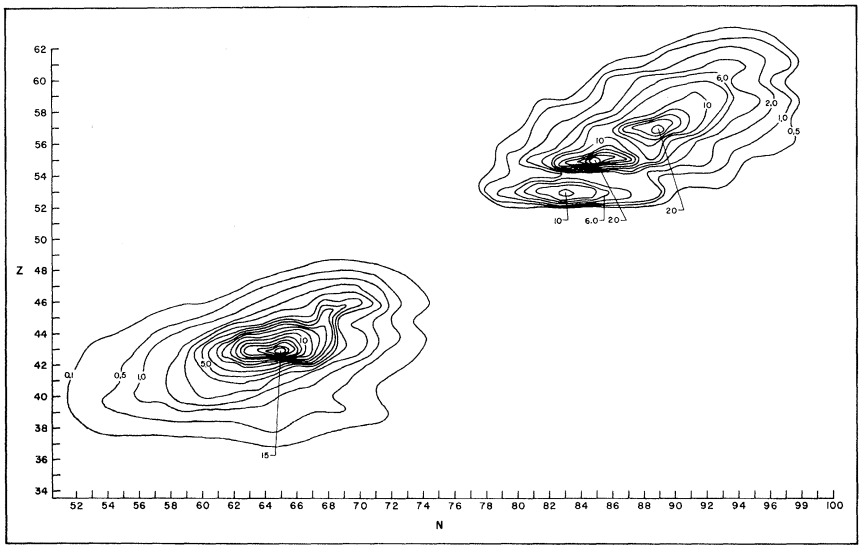

FIG. 4. A contour plot of the intensity of K x rays arising from fission fragments as a function of atomic number and neutron number (from Table I in units of 5×10^{-4} K x rays per fission).

the K x-ray yield distribution to the nuclear charge distribution, we begin by noting that the yield of K x rays from a fission fragment of atomic number Z and mass number A may be expressed as the product of a K x-ray emission probability $[C(Z,A)]$ and the fragment yield

$$Y^x(Z,A) = C(Z,A)Y(Z,A). \quad (1)$$

Since $C(Z,A)$ is an unknown quantity in this relationship, there is no way in which information pertaining to $Y(Z,A)$ may be obtained from measurements of $Y^x(Z,A)$ alone without making some assumption regarding $C(Z,A)$. It was seen in Fig. 4 that x-ray emission can be quite selective of particular nuclides, and hence one must exercise considerable care in these assumptions.

The K x-ray yields measured in the present experiment are not the yields of K x rays from fragments of specific mass and atomic numbers, but rather the yields of K x rays from fragments of specific atomic numbers averaged over a range of mass numbers. Hence Eq. (1) must be reformulated slightly to take into account the large dispersion associated with the mass determinations. In terms of the mass dispersion function, $d_A(M)$, which describes the yield distribution of fragments having

TABLE I. K x-ray intensity as a function of fragment mass interval and atomic number.

Light-fragment post-neutron-emission mass interval	Light-fragment atomic number (in units of 10^{-3} x ray per fission) 38	39	40	41	42	43	44	45	46	47	Total x rays per fission	Total x rays per fragment
91–93	0.31	0.39	0.27								1.05	0.063
93–95	0.33	0.50	0.58	0.26	0.11						1.86	0.081
95–97	0.37	0.67	0.95	0.52	0.36	0.18					3.05	0.106
97–99	0.38	0.83	2.04	1.18	0.82	0.39					5.72	0.132
99–101	0.40	0.64	2.96	2.53	1.90	1.07	0.36				9.85	0.156
101–103	0.54	0.72	2.69	3.82	4.24	2.72	0.97	0.16			15.9	0.178
103–105	0.38	0.70	1.71	3.85	6.81	7.03	1.90	0.46			22.9	0.203
105–107	0.24	0.50	0.65	2.21	6.87	12.5	4.79	0.71	0.10		28.6	0.221
107–109	0.38	0.50	0.56	1.16	4.36	15.1	8.56	2.46	0.51		33.6	0.264
109–111		0.36	0.34	0.59	1.47	9.31	10.6	3.70	1.47		28.0	0.243
111–113				0.13	0.55	3.61	7.08	4.16	2.63	0.56	18.8	0.191
113–115				0.10	0.21	1.04	2.45	2.56	4.71	1.37	12.4	0.164
115–117						0.27	0.69	0.95	4.17	2.16	8.35	0.169
117–119							0.17	0.13	1.14	1.02	2.52	0.119
119–121									0.20	0.20	0.43	0.074
121–123												
Total light-fragment intensities	3.39	5.90	12.8	16.5	27.8	53.4	37.7	15.3	15.0	5.44	193.2	

Heavy-fragment post-neutron-emission mass interval	Heavy-fragment atomic numbers (in units of 10^{-3} x ray per fission) 51	52	53	54	55	56	57	58	59	60	61	62	Total x rays per fission	Total x rays per fragment
131–133	0.91	0.54	2.03		0.30								3.83	0.084
133–135	0.89	0.42	7.14	0.53	1.39								10.4	0.135
135–137	0.76	0.24	9.94	1.80	5.44	0.74		0.12					19.0	0.213
137–139	0.72	0.48	8.19	3.67	13.5	2.60	1.00	0.26					30.5	0.290
139–141	0.88	0.55	4.29	3.53	20.5	5.89	3.64	1.17					40.4	0.350
141–143	0.69	0.61	2.19	2.40	17.2	10.7	8.58	1.67	0.25				44.4	0.374
143–145	0.31	0.41	0.88	0.97	10.1	11.9	16.3	4.08	1.45				46.4	0.396
145–147		0.10	0.57	0.82	3.74	7.50	18.6	9.32	4.15	0.41			45.2	0.386
147–149			0.34	0.50	1.20	2.69	11.5	12.5	8.32	2.36	0.59		40.1	0.570
149–151			0.26	0.44	0.46	1.16	4.43	9.62	10.5	4.81	1.67	0.66	34.0	0.742
151–153				0.30	0.37	0.71	1.68	4.60	8.48	7.67	2.89	1.04	27.8	0.909
153–155				0.21	0.21	0.52	0.81	1.84	4.36	8.00	4.48	1.75	22.2	0.974
155–157					0.11	0.13	0.31	0.67	1.28	3.84	3.70	2.13	12.2	0.884
157–159								0.18	0.25	0.88	1.28	1.30	3.89	0.549
159–161										0.14	0.26	0.38	0.78	0.23
161–163										0.13	0.13	0.13	0.33	0.22
Total heavy-fragment intensities	5.16	3.34	36.0	15.3	74.5	44.5	66.9	46.0	39.1	28.3	15.0	7.47	381.4	

mass number A as a function of mass interval, the measured yield of K x rays arising from fragments of atomic number Z and sorted into mass interval M is given by

$$Y^x(Z,M)=\sum_A Y^x(Z,A)d_A(M)$$
$$=\sum_A C(Z,A)Y(Z,A)d_A(M). \quad (2)$$

It was pointed out by Glendenin *et al.*,[4] that if the function $d_A(M)$ is broad compared to the width of a mass interval, then the detailed structural features of the yield of K x rays as a function of mass interval will be washed out and $Y^x(Z,A)$ will be averaged over a large number of isotopes. It is likely that, in general, the K x-ray emission probability $C(Z,A)$ does not vary rapidly from one isotope of a given nuclear type to the next (such as from one even-odd nucleus to the next even-odd nucleus of the same Z), and even though a large difference in the magnitude of $C(Z,A)$ may be expected in going from a nucleus of one nuclear type to the nuclear type of the immediately adjacent nuclei (such as from an even-odd nucleus to the two adjacent even-even nuclei), if the fluctuation from one isotope to the next is fairly constant and the dispersion function $d_A(M)$ sufficiently broad, then it is quite possible that the measured K x-ray distribution can be satisfactorily represented by replacing $C(Z,A)$ in Eq. (2) with an average K x-ray emission probability $\overline{C}_Z$ such that

$$Y^x(Z,M)\cong\overline{C}_Z\sum_A Y(Z,A)d_A(M). \quad (3)$$

It has been shown by Wahl *et al.*[8] that the isobaric yield distribution of fission products as a function of atomic number can be adequately described by the Gaussian distribution function

$$P_A(Z)=(1/\sqrt{2\pi}\sigma_Z)\,e^{-(Z_p-Z)^2/2(\sigma_Z)^2} \quad (4)$$

such that

$$Y(Z,A)=Y(A)P_A(Z), \quad (5)$$

where $Y(A)$ is the total yield of fragments of mass number A. It follows, therefore, that the isotopic yield distribution of fission fragments as a function of atomic mass number can similarly by formulated in terms of a smoothly varying distribution function $P_Z(A)$ defined by the relation

$$Y(Z,A)=Y(Z)P_Z(A), \quad (6)$$

where $Y(Z)$ is the total yield of fragments of atomic number Z. Although the function $P_Z(A)$ may deviate very slightly from a Gaussian because of small variations which occur in σ_Z from one mass chain to another, the most probable mass number A_p defined by the distribution function $P_Z(A)$ will correspond to the mass number of the most probable atomic number, Z_p, as defined by the distribution function $P_A(Z)$ in Eq. (4).

Returning to Eq. (3), it is seen that the total yield of K x rays from fragments of atomic number Z is obtained by summing over all mass intervals as follows:

$$Y^x(Z)=\sum_M Y^x(Z,M)=\overline{C}_Z\sum_M\sum_A Y(Z,A)d_A(M),$$

but

$$\sum_M\sum_A Y(Z,A)d_A(M)=Y(Z),$$

hence

$$Y^x(Z)=\overline{C}_Z Y(Z), \quad (7)$$

or

$$\overline{C}_Z=Y^x(Z)/Y(Z). \quad (8)$$

Substituting Eqs. (6) and (8) into Eq. (3) we obtain

$$Y^x(Z,M)=Y^x(Z)\sum_A P_Z(A)d_A(M). \quad (9)$$

The dispersion function was determined experimentally in Ref. 5 and found to be Gaussian. Thus

$$d_A(M)=Ne^{-(\bar{A}-A)^2/2(\sigma_d)^2}, \quad (10)$$

where $\bar{A}$ is the average mass number of fragments occurring in mass interval M. The average dispersion width, $\bar{\sigma}_d$, was 2.28 ± 0.42 amu for light fragments and 2.79 ± 0.41 amu for heavy fragments. (It is interesting to note that these experimental dispersion widths are considerably larger than those obtained by the method of Terrell[9] which typically gives values around $\sigma_d=1.7$ for measurements with a semiconductor fission fragment detector.) Since the dispersion function is symmetrical about the average mass of a given mass interval, its over-all effect will be to broaden the distribution of $Y^x(Z,M)$ without changing the position of its most probable value. Hence, within the limits of error imposed by the assumption that the K x-ray distribution can be represented by the average K x-ray emission probability $\overline{C}_Z$, the most probable mass associated with the emission of K x rays, A_p^x, may be taken as the centroid, A_p, of the P_Z distribution defined in Eq. (6). As has already been pointed out, the most probable mass, A_p, plotted as a function of Z should correspond identically to the curve obtained by plotting the most probable charge, Z_p, as a function of A.

The distributions obtained by plotting the $Y^x(Z,M)$ of Cs ($Z=55$) fission fragments versus $\bar{A}$ are shown in Fig. 5 for the full range - and three intervals - of total kinetic energy. It is seen that these distributions are smoothly varying and are well represented by Gaussians (solid curves), and that the widths of the distributions increase considerably from the highest total-kinetic-energy interval

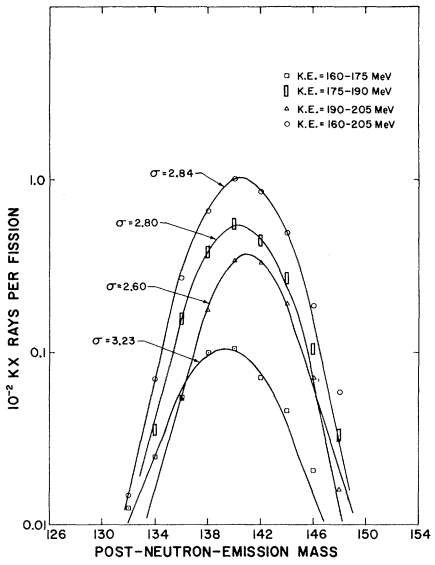

FIG. 5. The yield distributions of Cs K x rays as a function of average post-neutron-emission mass for several intervals of total kinetic energy.

(KE = 190 – 205 MeV) to the lowest total-kinetic-energy interval (KE = 160–175 MeV). This may be an indication that there is a larger neutron dispersion associated with the lower-total-kinetic-energy fission events from which the greatest numbers of neutrons arise.[10] All of the distributions of the type shown in Fig. 5 were fitted with Gaussian functions and in this way the centroids, A_p^x, and widths were obtained. The values of A_p^x for the K x-ray distributions containing the full range of total-kinetic-energy events are given in Table II. The average atomic numbers, Z_a^x, associated with the emission of K x rays from fragments of a given mass interval are listed in Table III as a function of the average fragment mass. These values were obtained by averaging the x-ray intensities shown in Fig. 3 and tabulated in Table I.

TABLE II. The most probable mass numbers associated with the emission of K x rays.

Z	A_p^x Post-neutron-emission	A_p^x Pre-neutron-emission
40	100.6 ±0.4	102.1
41	102.9 ±0.4	104.6
42	104.8 ±0.3	106.6
43	107.3 ±0.2	109.4
44	109.3 ±0.3	111.6
45	111.0 ±0.4	113.5
46	114.0 ±0.5	117.0
47	115.4 ±0.6	118.6
53	136.6 ±0.3	138.2
54	139.4 ±0.3	141.1
55	140.6 ±0.2	142.3
56	143.2 ±0.1	145.0
57	145.3 ±0.1	147.2
58	148.0 ±0.1	150.2
59	149.9 ±0.2	152.3
60	152.5 ±0.3	155.3
61	153.8 ±0.4	156.8
62	155.0 ±0.5	158.2

TABLE III. The average atomic numbers associated with the emission of K x rays.

Average post-neutron-emission mass number	Average pre-neutron-emission mass number	Z_a^x
92.0	93.6	39.0 ±0.3
94.0	95.6	39.6 ±0.2
96.0	97.6	40.1 ±0.2
98.0	99.5	40.4 ±0.2
100.0	101.5	41.0 ±0.1
102.0	103.6	41.5 ±0.1
104.0	105.8	42.1 ±0.1
106.0	107.0	42.6 ±0.1
107.9	110.1	43.1 ±0.1
109.9	112.3	43.6 ±0.1
111.9	114.6	44.3 ±0.1
113.9	116.8	45.2 ±0.2
115.8	119.1	45.9 ±0.3
132.1	133.0	52.5 ±0.5
134.0	135.2	53.1 ±0.3
136.0	137.0	53.7 ±0.2
138.0	139.6	54.4 ±0.2
140.0	141.7	55.0 ±0.1
142.0	143.7	55.5 ±0.1
144.0	145.8	56.2 ±0.1
145.9	148.0	57.0 ±0.1
147.9	150.2	57.8 ±0.1
149.9	152.3	58.5 ±0.1
151.9	154.6	59.1 ±0.1
153.9	156.9	59.7 ±0.2
155.8	159.4	60.3 ±0.2
157.8	161.9	60.8 ±0.3

IV. DISCUSSION

The acceptability of the A_p^x values obtained in Sec. III for representing the Z_p curve can be tested by checking to see how well they fulfill the requirement of charge and mass conservation. If the values of A_p^x are taken as corresponding to the values of A_p, then these most probable post-neutron-emission mass numbers, when transformed to pre-neutron-emission mass numbers, for complementary atomic number pairs (i.e., Z_L and Z_H pairs which fulfill the relationship $Z_L + Z_H = 98$) should sum to the mass number of the fissioning nucleus, 252. The average deviation from this sum for the pre-neutron-emission values of A_p^x listed in Table II is 0.3 amu. The deviation is, in all cases except one (for the pair $Z_L = 44$, $Z_H = 54$), within

experimental error and since it is highly unlikely that such consistency could be obtained if substantial biasing of the A_p^x values due to details of nuclear structure were occurring, we conclude that they must accurately represent the true values of A_p. Thus, it appears that the Z_p curve can in this way be adequately defined by K x-ray measurements.

The degree of consistency of the present data in fulfilling the requirements of charge and mass conservation is shown graphically in Fig. 6. In this figure are plotted the experimental values of pre-neutron-emission A_p^x versus Z separately for light and heavy fragments. The atomic-number and mass-number scales have been arranged such that complementary Z and A combinations intersect at the same relative positions on the two graphs. The solid line is an average of the light-fragment and heavy-fragment points obtained by superimposing the complementary Z and A points of the two graphs and drawing a curve passing equidistant between adjacent data points. The fact that the curve passes very close to all of the experimental points indicates that the charge and mass conservation requirements are fulfilled extremely well. Also shown in Fig. 6 are the experimental values of Z_a^x plotted versus pre-neutron-emission $\bar{A}$. The dashed line is the average curve passing through complementary pairs of these points. It is seen that very poor fulfillment of the requirement of charge and mass conservation is obtained for this set of data points. The apparent reason for this is that the atomic-number resolution is one Z unit, and hence there is no effective averaging of $C(Z,A)$ over Z in the determination of Z_a^x which would tend to smooth out the effects of specific features of nuclear structure.

Using the post-neutron-emission values of A_p^x, a curve was constructed from which the Z_p value for each mass chain could be read. These values of Z_p are listed in Table IV. The errors which are quoted for these numbers were determined graphically from the errors in the values of A_p^x. A comparison of these Z_p values with those determined previously by Glendenin and Unik reveals generally excellent agreement. In Table V are listed the differences between the Z_p values obtained here and those tabulated by Glendenin and Unik.[1] Only in the wings of the light-fragment distribution and for the average post-neutron-mass 139.6 do the two sets deviate by more than 0.2 charge units. The deviation at mass 139.6 is probably due to the biasing effect on the x-ray distribution of the accentuated yield of K x rays from ^{140}Cs (see Fig. 4), in which case we would expect our analysis to give the more accurate result.

The other parameter which is needed to completely specify the charge distribution is σ_Z. This width is related to the width of the $P_Z(A)$ distribution, and in principle it would be possible to determine σ_Z if the width of the A_p^x curve (the distribution of K x-ray intensities of a given Z as a function of A) and the width of the mass dispersion function, $d_A(M)$, could be measured to a sufficient degree of accuracy. In the present experiment, however, the average width of the A_p^x curve $\bar{\sigma}_A^x$, was 2.84 ± 0.05 amu for light fragments and 2.89 ± 0.11 amu for heavy fragments, which is of the same order of magnitude as the average width of the mass dispersion function $d_A(M)$. Thus the determination of the true widths of the A_p curves depends upon differences between numbers of nearly equal magnitude [(i.e., $\sigma_A = (\sigma_A^{x2} - \sigma_d^2)^{1/2}$] which means that relatively small errors in $\bar{\sigma}_A^x$ and σ_d become greatly magnified in the calculation of σ_A.

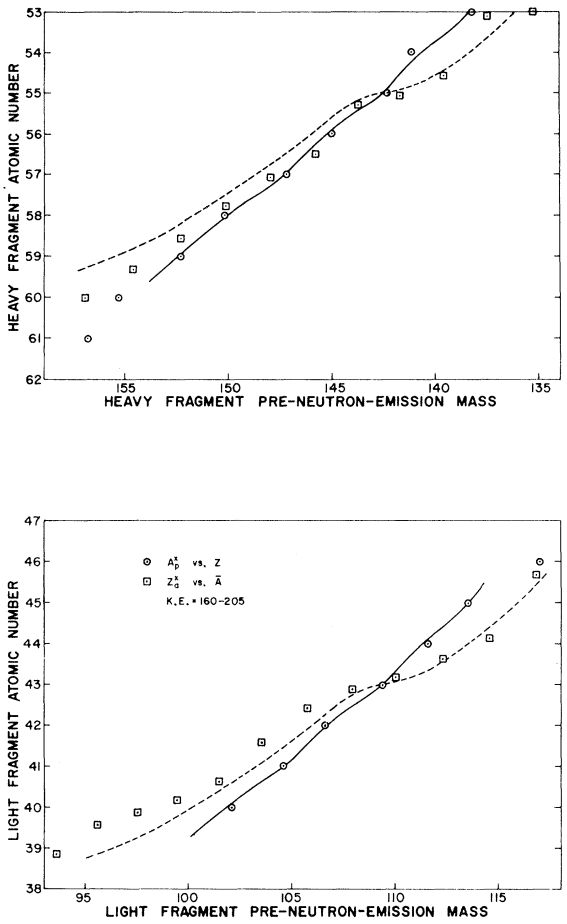

FIG. 6. The most probable pre-neutron-emission masses associated with the emission of K x rays (A_p^x) as a function of atomic number and the average atomic numbers associated with the emission of K x rays (Z_a^x) as a function of pre-neutron-emission mass. The solid and dashed lines represent averages of the respective complementary light- and heavy-fragment data points.

TABLE IV. Values of the most probable nuclear charge (Z_p).

Post-neutron-emission mass number	Z_p	Post-neutron-emission mass number	Z_p
100	39.2 ± 0.3	137	53.0 ± 0.2
101	40.2 ± 0.3	138	53.3 ± 0.2
102	40.6 ± 0.3	139	53.8 ± 0.2
103	41.1 ± 0.2	140	54.4 ± 0.2
104	41.6 ± 0.2	141	55.0 ± 0.1
105	42.0 ± 0.2	142	55.4 ± 0.1
106	42.5 ± 0.1	143	55.9 ± 0.1
107	43.0 ± 0.1	144	56.3 ± 0.1
108	43.4 ± 0.1	145	56.8 ± 0.1
109	43.9 ± 0.1	146	57.2 ± 0.1
110	44.4 ± 0.2	147	57.6 ± 0.1
111	45.0 ± 0.2	148	58.1 ± 0.1
112	45.4 ± 0.2	149	58.5 ± 0.2
113	45.7 ± 0.2	150	59.0 ± 0.2
114	46.0 ± 0.3	151	59.4 ± 0.2
115	46.7 ± 0.5	152	59.8 ± 0.2
		153	60.3 ± 0.3

Using the values presented here for $\bar{\sigma}_A^X$ and $\bar{\sigma}_d$ gives an error of the same order of magnitude as the calculated $\bar{\sigma}_A$. Unfortunately, the situation is not improved by reducing the mass dispersion since the smaller σ_d becomes, the worse becomes the representation of the A_p curve by the measured K x-ray intensities. We conclude, then, that high-resolution x-ray measurements are capable of providing accurate determinations of Z_p values, but that they are not likely to give reliable information regarding the width of the charge distribution.

Feather[11] has recently commented upon the differences he has observed between the even-odd fluctuations of K x-ray yield associated with binary fission and α-particle-accompanied ternary fission in the data of Watson, Bowman, and Thompson[3] and of Watson.[12] By defining the numerical parameter

$$P_K(Z)=\frac{[Y^X(Z)]^2}{[Y^X(Z-1)Y^X(Z+1)]} \tag{11}$$

(where Z is an even integer) to characterize these fluctuations, Feather examined the x-ray yields and found evidence for an over-all bias towards even-Z components in the spectrum of K x rays originating from fission accompanied by long-range α-particle emission.

We have adopted this same procedure [Eq. (11)] for the purpose of searching for correlated differences in the even-odd fluctuations of K x-ray yield as a function of total kinetic energy. The results of this analysis are shown in Fig. 7. (Only those values of P_K which were statistically significant in terms of their standard errors are shown.) The trend of the even-odd fluctuation for heavy fragments is the same for all three total-kinetic-energy intervals; namely the odd-even effect decreases as Z increases. This is consistent with the expectation of increased internal conversion in even-even nuclei as the rare-earth deformed region is penetrated. The same behavior is observed for the light-fragment atomic numbers 42 and 44. Comparing corresponding values of $P_K(Z)$ for the different intervals of total kinetic energy, it is seen in Fig. 7 that there is a definite enhancement of even-Z K x-ray contributions to the yields as the total kinetic energy increases. It has been pointed out by Thomas and Vandenbosch[13] on the basis of a comparison of maximum available excitation energies for odd-mass and even-even fragments that the formation of even-even fragments is strongly favored at low excita-

TABLE V. Comparison of Z_p values with those given by Glendenin and Unik.[a]

Average post-neutron-emission mass number	Z_p (present work) − Z_p (GU)
100.3	− 0.5
103.6	0.0
106.1	+ 0.1
108.8	0.0
111.9	− 0.2
114.7	+ 0.6
136.8	+ 0.1
139.6	+ 0.6
143.1	0.0
146.6	− 0.2
149.9	+ 0.1
152.9	+ 0.2

[a]See Ref. 1.

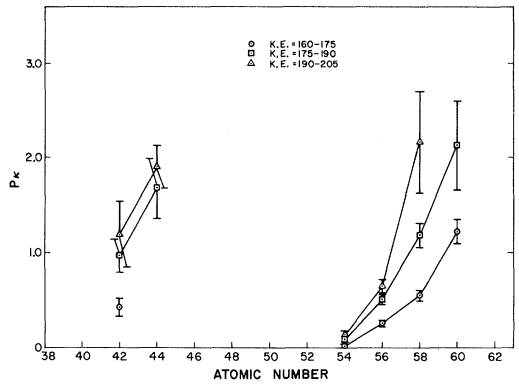

FIG. 7. The K x-ray-yield fluctuation parameter $[P_K(Z)]$ for even-Z fragments.

tion or high kinetic energies. The observed enhancement of the K x-ray yields for even-Z products experimentally verifies this expectation. In view of this effect, it would appear that the charge distribution should change markedly as a function of total kinetic energy and that this change should be observable in the A_p values.

Graphs of Z versus A_p^x, similar to those shown in Fig. 6, are presented in Fig. 8 for three intervals of total kinetic energy. It is apparent that the A_p^x values undergo substantial shifting from one total-kinetic-energy interval to the next and that this effect is largest for the light fragments. The solid line in the heavy-fragment graph represents the best average of the data points for the three total-kinetic-energy intervals and the solid line in the light-fragment graph is a superposition through complementary (Z,A) combinations of the heavy-fragment line. As can be seen from these lines, the data points do not fulfill the requirements of charge and mass conservation very satisfactorily. It is therefore questionable as to whether or not the observed A_p^x shifts are really attributable to changes in the primary charge distribution since, in this event, similar behavior would be expected for complementary fragments. An alternative explanation might be that the neutron data of Bowman *et al.*[10] and the formulation by Takekoshi and Thompson,[14] which we have used to transform the measured fragment kinetic energies into fragment masses (see Ref. 5), do not accurately represent the kinetic energy dependence of neutron emission. Erroneous neutron corrections could

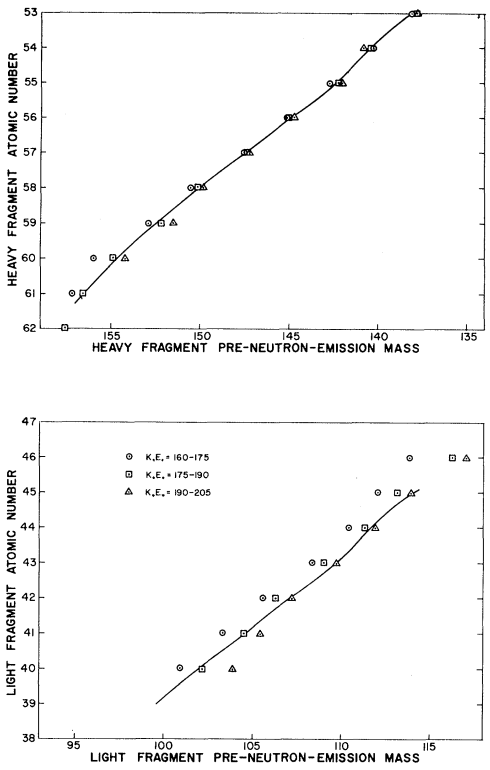

FIG. 8. The most probable pre-neutron-emission masses (A_p^x) as a function of atomic number for three intervals of total kinetic energy. The solid lines represent an average of the heavy-fragment data points.

shift the A_p^x values in either direction; that is the heavy-fragment A_p^x values could be erroneously shifted in such a way as to cause them to closely overlap each other and thus cover up any real shift, or conversely the light-fragment A_p^x values could be shifted apart giving the appearance of a real shift. Further investigation will be required before this question can be resolved.

V. ACKNOWLEDGMENTS

We wish to express our gratitude to Dr. J. B. Natowitz, Dr. J. B. Wilhelmy, Dr. E. Chulick, and Dr. E. Cheifetz for many helpful discussions and suggestions, and to Mrs. Janis Scherer, Robert Howard, and James Sjurseth for their invaluable help in analyzing the data.

†Work at University of California Lawrence Radiation Laboratory supported by U. S. Atomic Energy Commission. Work at Texas A & M University supported in part by the U. S. Atomic Energy Commission and the Robert A. Welch Foundation.

[1]L. E. Glendenin and J. P. Unik, Phys. Rev. 140, B1301 (1965).

[2]S. S. Kapoor, H. R. Bowman, and S. G. Thompson,

Phys. Rev. 140, B1310 (1965).
[3]R. L. Watson, H. R. Bowman, and S. G. Thompson, Phys. Rev. 162, 1169 (1967).
[4]L. E. Glendenin, H. C. Griffin, W. Reisdorf, and J. P. Unik, in Proceedings of the International Atomic Energy Agency Symposium on Nuclear Fission, Vienna, Austria, July, 1966 (to be published), paper No. SM-122/114.
[5]R. L. Watson, J. B. Wilhelmy, R. C. Jared, C. Rugge, H. R. Bowman, S. G. Thompson, and J. O. Rasmussen, Nucl. Phys. A141, 449 (1970).
[6]J. S. Fraser, Physics and Chemistry of Fission, (International Atomic Energy Agency, Vienna, Austria, 1965), Vol. I, p. 451.
[7]S. R. Dolce, W. M. Gibson, and T. D. Thomas, Phys. Rev. 180, 1177 (1969).
[8]A. C. Wahl, R. L. Ferguson, D. R. Nethaway, D. E. Troutner, and K. Wolfsberg, Phys. Rev. 126, 1112 (1962).
[9]J. Terrell, Phys. Rev. 127, 880 (1962).
[10]H. R. Bowman, J. C. D. Milton, S. G. Thompson, and W. J. Swiatecki, Phys. Rev. 126, 2120 (1963); 129, 2133 (1963).
[11]N. Feather, Phys. Rev. (to be published).
[12]R. L. Watson, Phys. Rev. 179, 1109 (1969).
[13]T. D. Thomas and R. Vandenbosch, Phys. Rev. 133, B976 (1964).
[14]E. Takekoshi and S. G. Thompson, University of California, Lawrence Radiation Laboratory Report No. UCRL-17299, 1967 (unpublished).

PHYSICAL REVIEW C VOLUME 1, NUMBER 5 MAY 1970

Comments and Addenda

The Comments and Addenda section is for short communications which are not of such urgency as to justify publication in **Physical Review Letters** *and are not appropriate for regular Articles. It includes only the following types of communications: (1) comments on papers previously published in* **The Physical Review** *or* **Physical Review Letters**; *(2) addenda to papers previously published in* **The Physical Review** *or* **Physical Review Letters**, *in which the additional information can be presented without the need for writing a complete article. Manuscripts intended for this section may be accompanied by a brief abstract for information-retrieval purposes. Accepted manuscripts will follow the same publication schedule as articles in this journal, and galleys will be sent to authors.*

Theories of Isobaric Analog Resonances

Hans A. Weidenmüller
Institut für theoretische Physik der Universität und Max-Planck-Institut für Kernphysik, Heidelberg, West Germany
(Received 4 December 1969)

The differences between various microscopic theories of isobaric analog resonances are exhibited. It is shown that the physical assumptions underlying the recent theory of Zaidi and Dyer are identical to those used in the formulation of Mekjian and MacDonald.

The present note comments upon a recent paper by Zaidi and Dyer.[1] In this paper, a theory of isobaric analog resonances is presented which is claimed[1] to give results different from those obtained both by Mekjian and MacDonald[2] and by the present author.[3] It is the purpose of the present note to exhibit the differences between the theories of Refs. 2 and 3, and to show that the theory of Zaidi and Dyer[1] uses the same physical picture as that of Mekjian and MacDonald.[2] It is also shown that the formulas for the averaged S matrix elements obtained in Ref. 1, when modified so as to make them consistent with the assumptions used in deriving them, are the same as the formulas given in Ref. 2.

The theories of Refs. 1–3 are based upon a shell-model approach to nuclear reactions. The single-particle Hamiltonian h_0 contains the kinetic energy of the particle and some suitably chosen average potential. In Refs. 1–3, the single-particle potential for the neutrons is chosen to be the average Hartree-Fock potential. (In Ref. 1, this potential is then approximated by a Woods-Saxon potential with a Thomas-type spin-orbit term, but this is irrelevant for what follows.) References 2 and 3 differ in the choice of the single-particle potential for the protons. In Ref. 3, this potential is chosen to be identical to that for the neutrons, except that the average Coulomb field is added. In Ref. 2, on the other hand, the proton potential is the sum of the Coulomb potential and a single-particle potential which differs by the symmetry potential from that of the neutrons. Because of this different choice of the single-particle potential for the protons, the residual interactions employed in the two theories (the two-body interactions minus the